MULTIPHASE PUMPING WITH TWIN-SCREW PUMPS— UNDERSTAND AND MODEL HYDRODYNAMICS AND HYDROABRASIVE WEAR

by
Gerhard Vetter
Professor
Wolfgang Wirth
Research Engineer
Heiko Körner
Research Engineer
and
Sabine Pregler
Research Engineer
Institute of Apparatus and Chemical Machinery
University of Erlangen-Nuremberg
Erlangen, Germany

Gerhard Vetter accepted a chair (professorship) for Apparatus and Chemical Machinery at the University of Erlangen-Nuremberg, in Erlangen, Germany, in 1981. He has dedicated 40 years to research, development, and design of pumps and metering equipment. He has been one of the pioneers in diaphragm pump development. Many papers, patents, and contributions to textbooks, some dealing with basics like cavitation, fatigue, pulsation, vibrations, abrasive wear, and metering accuracy, have established his reputation as a pump specialist.

Dr. Vetter obtained his Dipl.-Ing. degree (Mechanical Engineering) at Technische Universität Karlsruhe, Germany. After some years as a Research Engineer in turbomachinery there, he joined Lewa, Leonberg, Germany, as head of the R & D Department. He became Chief Engineer and Technical Managing Director before joining the University of Erlangen-Nuremberg. Dr. Vetter is also a Corresponding Advisory Committee Member of the International Pump Users Symposium.

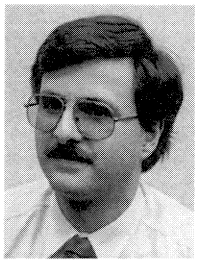

Wolfgang Wirth is a Staff Member and Research Engineer for the Institute of Apparatus and Chemical Machinery at the University of Erlangen-Nuremberg, in Erlangen, Germany.

Dr. Wirth obtained his Dipl.-Ing. degree (Chemical Engineering, 1986) at the University of Erlangen-Nuremberg, Germany. As a Research Engineer, he prepared a thesis about methods for modeling the hydraulic and tribologic properties of progressing cavity pumps and received his Dr.-Ing. degree in 1993.

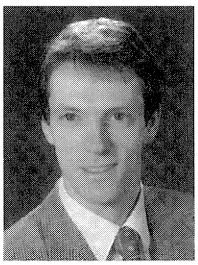

Heiko Körner is a Research Engineer for the Institute of Apparatus and Chemical Machinery at the University of Erlangen-Nuremberg, in Erlangen, Germany.

Dr. Körner obtained his Dipl.-Ing. degree (Chemical Engineering, 1993) at the University of Erlangen-Nuremberg, Germany. As a Research Engineer, he performed a doctoral thesis in 1998 about conveying multiphase fluids with twin-screw pumps.

ABSTRACT

Crude oil and gas production can be enhanced by multiphase pumping from the well subsea to far distant production platforms. The twin-screw pump has proven quite suitable for this application. The positive displacement principle offers efficient multiphase performance within a wide range of gas void fractions and can handle hydroabrasive conditions fairly well, too.

The paper reports about modeling the hydrodynamic performance and hydroabrasive wear of twin-screw pumps. The influence of the gas void fraction on the pump capacity can be modeled by the "disc model" and assumptions about the fluid conditions in the internal pump clearances. The model implemented into a computer program will be verified by experimental testing of various pump features with respect to performance, pressure distribution, thermodynamics, and bending deflection of the screw shafts.

The phenomena of the hydroabrasive wear will be studied by the rotary clearance tribometer as well as with pump field tests with silica sand/water suspensions. Based on a number of material combinations including hard coating on tungsten carbide basis, the relative suitability of materials as well as the local wear phenomenology will be analyzed.

The paper offers a full survey about the hydroabrasive twin-screw pump wear characteristics and steps to predict and achieve satisfactory pump life.

INTRODUCTION

Multiphase pumping of crude oil/natural gas/water-mixtures as being delivered from the wellheads to far distant processing plants is a step to promote economic crude oil and gas production.

As the subsea exploitation in total will grow faster and faster in the future (expected yield around 40 percent until 2010 from subsea locations), and as the investment for the platforms is progressively increasing with the depth of subsea locations of the wellheads, multiphase pumping will offer attractive chances to improve economy.

When placing multiphase pumps at the wellheads, fields can be exploited more efficiently, especially smaller ones. The oil/gas-discharge can be conveyed either directly onshore or to platforms at a far distance for further processing, thus avoiding a higher number of expensive separate platforms. In very deep waters—locations of around 1000 m depth actually being envisaged—the hydraulic conditions offer more efficient exploitation due to the pressure conditions involved. One feature of application is shown in Figure 1. The subsea multiphase pumping package located directly at the wellhead and connected with control and supply circuits is conveying the multiphase fluid mixture to a far distant central platform or, as an alternative, straight onshore for further processing.

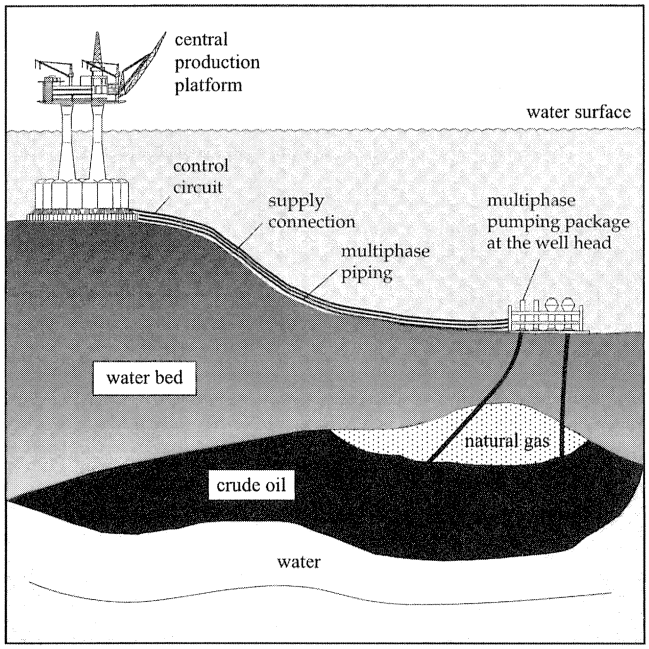

Figure 1. Multiphase Pumping for the Oil/Gas Production Subsea/Offshore.

Multiphase pumping is not only an enhancing step for the concentration of processing from a number of wellhead supplies, but, due to the additionally implemented pressure, an effective promotion of the exploitation and transportation procedure, including savings in equipment and operating costs.

The multiphase pumping units must be able to handle fluids from around 100 percent of gas to 100 percent of liquid in all fractions and varying from field to field, as well as during the exploitation period. Slugs of liquid or gas represent a challenge for the pump with respect to thermodynamic and dynamic operating conditions. Furthermore, the fluid mixture may exhibit corrosive, viscous, and abrasive elements due to the water, oil, gas, and particle fractions. The hydraulic operating conditions for multiphase oil/gas processing range in capacity from up to 1200 m^3/h and in differential (total) pressure up to 80 (100) bar, depending on the distance of transportation and the pressure and productiveness of the well.

Actually, special features of multistage helical (turbo) pumps (Cordner, 1994; de Salis, 1997) and of twin-screw (positive displacement) pumps (Prang, 1981; Dal Porto and Larson, 1996; Neumann, 1992; Granato, et al., 1998) are competing in small numbers of multiphase onshore and some offshore subsea applications. The twin-screw pumps (Figure 2) have proven quite suitable for multiphase fluids pumping, as their performance exhibits typical positive displacement characteristics. The fluid is transported, enclosed in serially acting chambers locked by clearance seals between the meshing screws (left-/right-hand screws, single/double threaded).

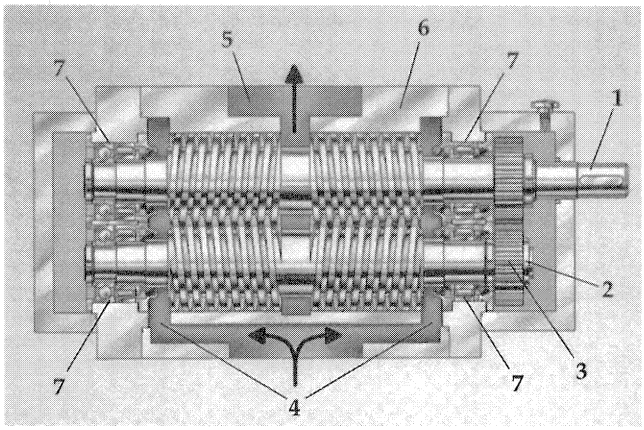

Figure 2. Double Flow Twin-Screw Pump with External Bearings and Gear. (1. Driving shaft; 2. Driven shaft; 3. Gear; 4. Suction; 5. Discharge; 6. Housing; 7. Bearings) (Courtesy of Körner, 1998)

The double-flow layout where the screw package pumps from the ends to the middle, offers advantages of: doubling capacity, balancing the axial hydraulic thrust, and avoiding shaft seals loaded by high pressure.

The screws (which can be flexible), designed according to the requirements with respect to head and flow, mesh but do not transmit torque mutually. For this purpose, the screws are driven by an external timing gear and therefore are kept within a mutual distance by clearances enabling the pumps to also convey fluids contaminated with particles.

Twin-screw pumps operate at relatively low velocities and can be custom designed with regard to pitch, screw length or number of chambers, clearances, number of threads, screw profiles and diameters, material selection, housing, and speed. Flexible design to meet user's requirements and linear control characteristics with speed represent countless advantages of the twin-screw pump types.

The essential topics to be considered during the selection of multiphase screw pumps are the reduction of the leak losses through the functional internal clearances and their protection against hydroabrasive wear.

Three locations (Figure 3) within the screw package have to be distinguished:

- Circumferential clearance (CC) between the screw peripheral diameter and the housing,
- Radial clearance (RC) between the internal and the external diameter of the screw profile, and
- Flank clearances (FC) between the flanks of the screw profile.

The dimensions of the clearances depend on the machining tolerances, the stiffness of the screws, the housing structure against elastic deformation by the pressure, as well as the play involved with the bearings. The circumferential clearances (CC) are of dominating influence on the internal leak losses as their cross section is by far the largest one (eight-shaped as shown in Figure 3(b)).

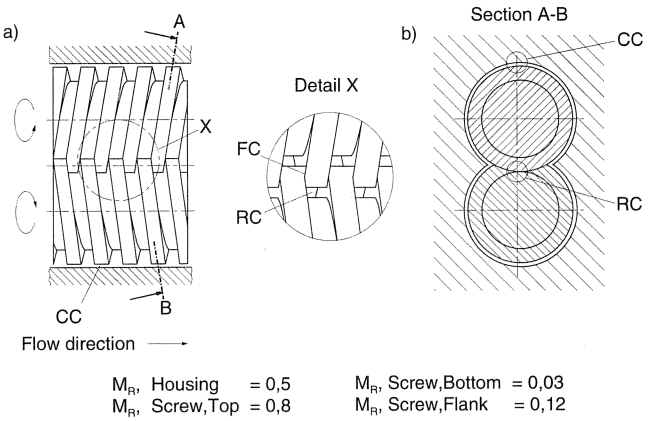

Figure 3. Sealing Clearances and Meshing Ratio (M_R).

The crucial point to reduce the internal leak losses for multiphase pumping is to promote the clearances to be filled by liquid to the highest achievable extension. Some further important topics are: small clearance dimensions (limited to > 100 µm due to tolerances), and sufficient number of locks (or length of the screw) in order to keep the pressure differentials at the individual clearance locations low (multistaging).

During oil/gas multiphase pumping where the fluids are usually contaminated by abrasive particles, the tribological systems involved, characterized by sliding and jetting wear, should be considered (Figure 4). Despite all attempts to segregate the particles, the fluid contains smaller and larger particles as well as particles of a magnitude that are jammed and crashed within the clearances (Figure 4, left). The smaller particles will cause jetting wear, those of the magnitude of the clearance dimensions, sliding wear, and the larger ones will be rejected.

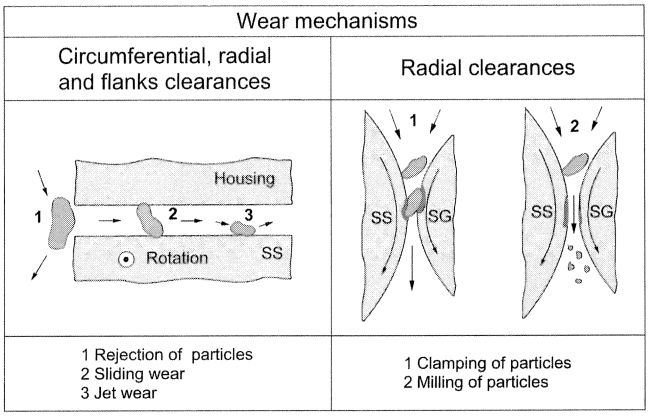

Figure 4. Wear Mechanisms in the Sealing Clearances.

This is true for the more or less parallel clearances (CC, FC). For the radial clearances (RC), additional milling or crashing wear action (Figure 4, right) of the particles, implementing further variations of the tribosystem, should be expected.

A very meaningful parameter for the hydroabrasive wear intensity at clearances is represented by the meshing ratio, M_R. This is the fraction of the total time period related to that during which a surface element of the wearing parts is really meshing with its counterpart. The M_R data in Figure 3 clearly demonstrate that the circumferential clearances (CC) exhibit the highest meshing ratio (M_R = 0.8); this means that much attention should be paid to wear prevention at these locations.

As the wear rate greatly depends on the hardness ratio between the particles and the relevant parts, as well as the particle concentration and size distribution, wear prediction should be based on the definite analysis of the fluid properties (Vetter, et al., 1996).

The following report is the result of an extended joint study of the University of Erlangen and Leistritz Nuremberg about the hydrodynamic design and the wear protective steps for multiphase twin-screw pumps. A number of pumps have proven their suitability for oil/gas onshore and offshore production, since the first subsea feature (500 m^3/h, suction/discharge pressure 20/80 bar, 660 m water depth) should be installed by now (Wincek and Moser, 1999; NN Westinghouse Electric Co., 1999).

HYDRODYNAMIC PERFORMANCE OF MULTIPHASE TWIN-SCREW PUMPS

When considering hydraulics and hydrodynamics during multiphase pumping with twin-screw pumps, the problem can be reduced to a two-phase fluid. The term multiphase comes from the fractions—oil/gas/water/particles—of the fluid mixture. But as the particle fraction stays far below one percent, there remain only two homogenous phases—oil/water (rather close in viscosity at the temperatures involved) and gas.

Although twin-screw pumps have been applied for two-phase gas/liquid-mixtures for a long time, it took the last 15 years to develop a suitable theoretical approach for a reliable computational performance prediction (Christiansen, 1986; Vetter and Wincek, 1993a, 1993b; Wincek, 1992; Körner, 1998). The modeling of twin-screw pumps for operation with liquids was developed much earlier (Hamelberg, 1968), however.

Twin-Screw Pumps Theory

The pump's total capacity, $\dot{V}$ (suction flow), represents the difference between the geometrical (theoretical) displacement, $\dot{V}_{geo}$, capacity and the total internal leak flows, $\dot{V}_L$ (comprising the four flows from two screws, double flow layout) (Wincek, 1992):

$$\dot{V} = \dot{V}_{geo} - \dot{V}_L \tag{1}$$

The geometrical displacement flow, $\dot{V}_{geo}$, depends on the geometry of the screw package and the speed of the pump.

$$\dot{V}_{geo} = f(D,d,a,h,G,n) \tag{2a}$$

$$\dot{V}_{geo} = V_u \cdot n = A \cdot h \cdot n \tag{2b}$$

In fact, $\dot{V}_{geo}$ can also be evaluated with the displacement volume per revolution, V_u, or with the flow cross-section, A, multiplied with the pitch, h, of the screw. The total internal leak flow consists of the contributions of all internal sealing clearances involved (Figure 3, CC, RC, FC).

Leak Flow Through the Sealing Clearances

In principle, the flow is of the Couette-type as the surfaces defining the shape and dimensions of clearance are in relative motion superimposed by a pressure differential driven share. The flow rate through an individual sealing clearance, $\dot{V}_c$, basically consists of a first component driven by the pressure differential, $\dot{V}_{cd}$, and a second one due to the rotational meshing, $\dot{V}_{cr}$:

$$\dot{V}_c = \dot{V}_{cd} + \dot{V}_{cr} \tag{3}$$

The general assumptions for modeling the flow rate through liquid-filled clearances are:

- Newtonian fluid behavior
- Stationary flow, fully developed

- Entry and exit losses neglected
- Hydraulically rough clearance surfaces
- Additional losses involved by the superimposition of the differential pressure and rotational component are neglected

The three types of clearances involved have been investigated together with experimental verifications by Vetter and Wincek (1993a, 1992). The Tables 1 and 2 provide a survey about the basic theory of the clearance flow rate evaluation. In order to illustrate the clearances and flow conditions as well, some further assumptions are shown in Figures 5, 6, and 7. All the clearances are relatively narrow compared with their length.

Table 1. Differential Pressure Components of the Leak Flows.

clearance	flow-mode	volume flow	
circumferential clearance (CC)	laminar	$\dot{V}_{L,D} = \frac{\Delta p \cdot l_{CC} \cdot s_{CC}^3}{12 \cdot B \cdot \rho \cdot \nu}$	(4)
	turbulent	$\dot{V}_{L,D} = l_{CC} \cdot s_{CC} \cdot (2 \cdot \lg \frac{2 s_{CC}}{K} + 0{,}97) \cdot \sqrt{\frac{4 \cdot \Delta p \cdot s_{CC}}{B \cdot \rho}}$	(5)
radial clearance (RC)	laminar	$\dot{V}_{L,D} = \frac{\Delta p \cdot B}{12 \cdot \rho \cdot \nu \cdot \int_0^{2x_0} \frac{1}{s_{RC}(x)^3} dx}$	(6)
	turbulent	$\dot{V}_{L,D} = \frac{2 \cdot B \cdot \sqrt{\Delta p}}{\sqrt{\rho \cdot \int_0^{2x_0} \frac{1}{(2 \cdot \lg \frac{2 \cdot s_{RC}(x)}{K} + 0{,}97)^2 \cdot s_{RC}(x)^3} dx}}$	(7)
flank clearance (FC)	laminar	$\dot{V}_{L,D} = \frac{\Delta p \cdot H \cdot s_{FC}^3}{24 \cdot l_f \cdot \rho \cdot \nu}$	(8)
	turbulent	$\dot{V}_{L,D} = H \cdot s_{FC} \cdot (2 \cdot \lg \frac{2 s_{FC}}{K} + 0{,}97) \cdot \sqrt{\frac{\Delta p \cdot s_{FC}}{l_{FC} \cdot \rho}}$	(9)

Table 2. Rotational Components of the Leak Flows.

clearance	volume flow	
circumferential clearance (CC)	$\dot{V}_{L,R} = s_{CC} \cdot l_{CC} \cdot \frac{R^2 \cdot \omega}{R_H - R} \cdot \left[\ln\left(\frac{R_H}{R}\right) \cdot \left(1 + \frac{R^2}{R_H^2 - R^2}\right) - \frac{1}{2} \right] \cdot \sin\left(\arctan \frac{h}{D \cdot \pi}\right)$	(10)
radial clearance (RC)	$\dot{V}_{L,R} = B \cdot s_0 \cdot \frac{\omega \cdot R + \omega \cdot r}{2}$	(11)
flank clearance (FC)	$\dot{V}_{L,R} = H \cdot s_{FC} \cdot \frac{\omega \cdot (R + r)}{2}$	(12)

Circumferential Clearance

The circumferential clearance is considered annular with an interruption in the meshing area (refer to Figure 3(b)). With respect to the leak flow contribution, the circumferential clearance is the most effective one. From Figure 5, the superimposed two contributions can be understood. The differential pressure component represents the flow in the ξ-direction (orthogonal to the flight of the screw, Figure 5(a)).

The velocity distribution of the Couette-flow provides a component in the flow-direction ξ, too, and induces the flow profile as shown in Figure 5(b).

If assuming annular clearances, the real leak losses will be slightly larger as the screws will be deflected by the bending forces due to the pressure distribution, and will therefore exhibit eccentrically. This influence is taken into account by evaluating the elastic deformations and implementing adequate correcting algorithms for the eccentric clearance flow (Wincek, 1992; Vetter and Wincek, 1993b). The method has been verified by experimental investigations.

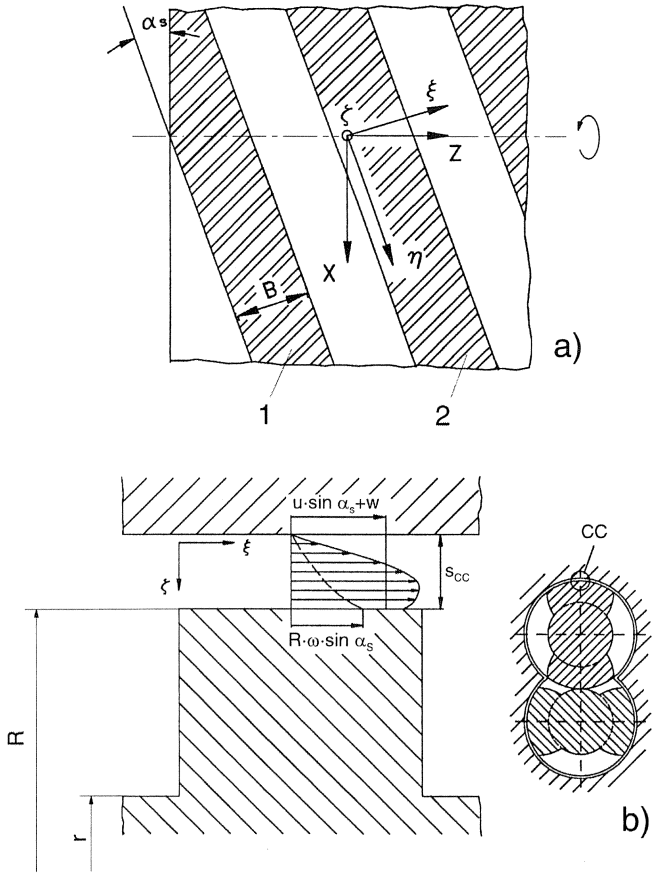

Figure 5. Flow in the Circumferential Clearance. (1. Outside diameter of the screw; 2. Internal diameter)

Radial and Flank Clearances

The flow through the radial clearances (RC) is similar but not the same as that of circumferential (CC), because the geometrical profile is curved and therefore the pressure distribution in the flow direction is not linear (Figure 6). Accordingly, the method of calculation is more complex as the effective clearance length, $2 \cdot x_0$, must be evaluated by iteration.

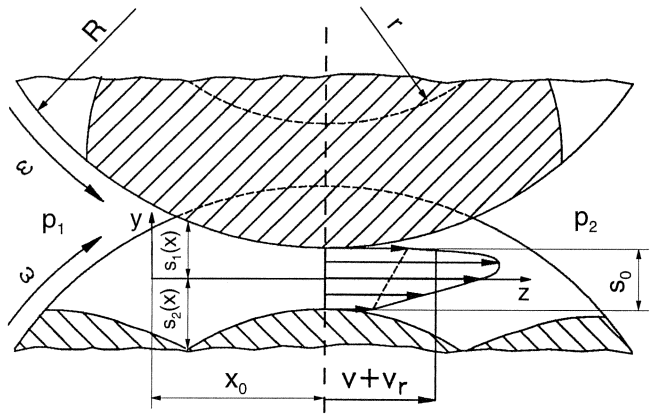

Figure 6. Radial Clearance Flow of a Screw Pump.

For modeling the flank clearances (FC), the difficulties connected with the shape and geometry can be solved by substituting the real clearance by an assumed one with the width of half the chamber depth, $H/2$, and a fictive length, l_f, so that the area, F, remains the same in total (Figure 7).

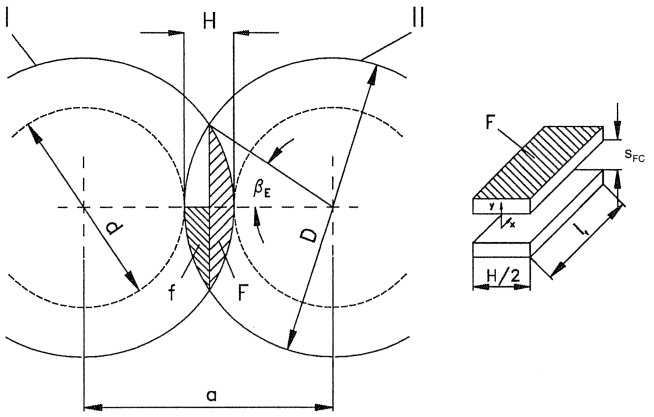

Figure 7. Fictive Clearance Dimensions for the Approximation of Flank Clearances.

Modeling the Pump

The basic idea of the multiphase twin-screw pump's operation can be explained with the circular disc-model (Figure 8). The chambers between the discs are moving (like an infinite chain) through the pump's housing and transporting the fluid enclosed within the chambers from the suction to the discharge against the required pressure differential.

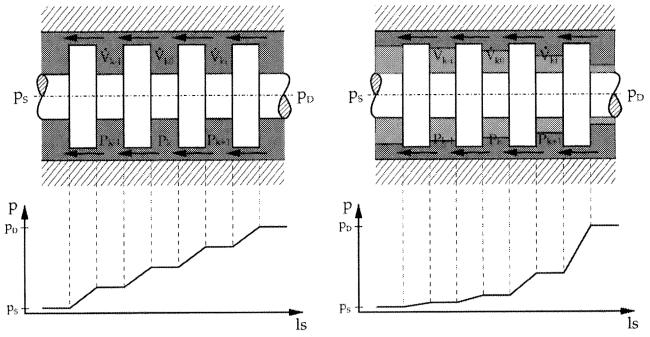

Figure 8. Circular Disc Model for Screw Pumps. (Left: Liquid pumping; Right: Two-phase pumping)

During single-phase (liquid) operation (Figure 8, left), the leak flow through the clearances will exhibit approximately constant as the clearance cross section will stay constant, too, although slight effects through eccentricity may happen. As a consequence, the pressure distribution will stay linear (liquid compressibility constant and very low).

During two-phase gas/liquid operation (Figure 8, right) the gas/liquid-mixture will separate under the action of the centrifugal forces, the gas staying in the center and the liquid in the circumferential area filling the clearances and keeping them "tight." The compression of the gas again is effected by the balance of the two-phase fluid displacement and single-phase backward directed leak flows. As the compressibility of the gas is neither constant nor low, the pressure distribution basically does not yield linearly and demonstrates larger gradients toward the discharge end (Figure 8, right). The pump model, as explained, must be amended, in order to cope with reality, by two major steps.

Fluid Sealing in the Clearances

A closer look (Figure 9) clearly shows that, due to the meshing of the screws, it must be expected that the rotational symmetry of the liquid/gas separation and the liquid filling of the clearances will be disturbed more and more with growing gas void fractions most probably ending with a homogenous gas/liquid mixture (foam).

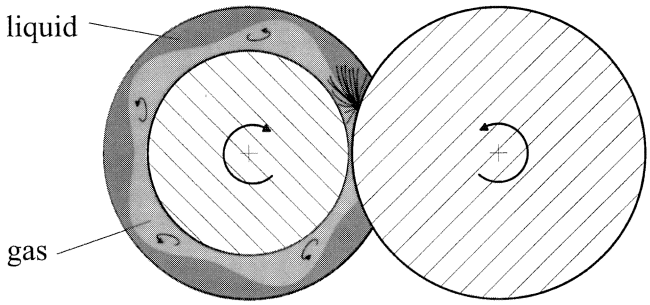

Figure 9. Disturbances of the Liquid Ring.

From various experimental studies, it is known that up to a gas fraction of around 85 percent at the suction side, the pump system is obviously behaving in a way that all the clearances are staying filled with liquid. This means (Figure 9) that the fluctuating liquid ring is still thicker than the width of the circumferential clearance and that the flank and radial clearances permanently encounter liquid swept into their cross-sections. The physical evidence of this assumption appears quite plausible, as, within the meshing area, the flanks and radial clearances will be submerged by the liquid due to the local impact pressure involved.

With a growing gas fraction above 85 percent, the two phases will not separate any more but mix to a quasihomogenous foam by spraying. Based on this assumption, the modeling of the leak losses through all clearances has been adapted accordingly. Viscosity, μ, and density, ρ, are now calculated for a homogenous gas/liquid-mixture instead. The comparison of experimental and computational results has stimulated the application of the algorithm by Ciccetti and Lombard (1960), which is quite suitable to satisfactorily cope with reality. It should be clearly understood that the selected method to improve the modeling quality of multiphase twin-screw pumps in the range of very high gas fractions represents a kind of empirical step. The mean density, ρ_{ch}, and viscosity, μ_{ch}, of the two-phase fluid in a relevant chamber are subsequently modeled as follows:

$$\rho_{ch} = \frac{\alpha \cdot \rho_g + (1 + \alpha)\, \rho_{liq}}{\alpha \cdot \frac{\rho_s}{\rho_{ch}} + (1 - \alpha)} \tag{13}$$

$$\mu_{ch} = \frac{\alpha \cdot \rho_g \cdot \mu_g + (1 - \alpha)\rho_{liq} \cdot \mu_{liq}}{\alpha \rho_g + (1 - \alpha)\rho_{liq}} \tag{14}$$

It is assumed that $\rho_{ch} = \rho_c$ and $\mu_{ch} = \mu_c$, where the data with the index, c, represent those existing in average within the relevant sealing clearances.

The Real Pump Model

The simplified model (Figure 8) requires some amendments in order to better cope with the pump's reality. The real screw package—depending on the type of layout—does not only demonstrate serial but also parallel leakage flows and the analysis of the various leakage flows has to be modeled according to the screw layout concerned.

The method will be explained for the example of a double-thread three-stage (chamber) twin-screw pump as it has been applied for the studies. For other pump layouts, the methodology can be applied accordingly but not identically.

The choice of the screw spindle profile and layout is flexible for screw-pumps in order to cope best with the application case: long multistage stiff screws for high pressure or low viscous liquids, short screws with large flow cross section for high viscosity low pressure cases, etc.

The stage represents the smallest displacement unit consisting of the chamber locked by the sealing clearances. The growing number of stages, k, provides more sealing clearances against the total pressure difference and decreases the total leak flow (dimensionless rotor length, λ_l):

$$k = G \cdot \frac{\lambda_l + \beta}{\pi} - G + 0.5 \tag{15a}$$

$$\lambda_l = \frac{l_s}{h} \tag{15b}$$

As usual, the number of stages, k, yields a decimal number (g, number of full stages; δ, fractions of a stage; $k = g + \delta$). It is necessary to distinguish the screw action within two ranges of the full angle of rotation, φ:

- $0 < \varphi < 2\pi\delta/G$—The screw action yields as if it had g chambers, but $g + 1$ circumferential clearances (locks).
- $2\pi\delta/G < \varphi < \pi\delta/G$—The screw action yields as if it had $g - 1$ chambers, but g circumferential clearances only.

The circular disc-model explained earlier has to be adapted to the double-thread layout according to Figure 10, the leak flows flowing and compressing the gas fraction accordingly.

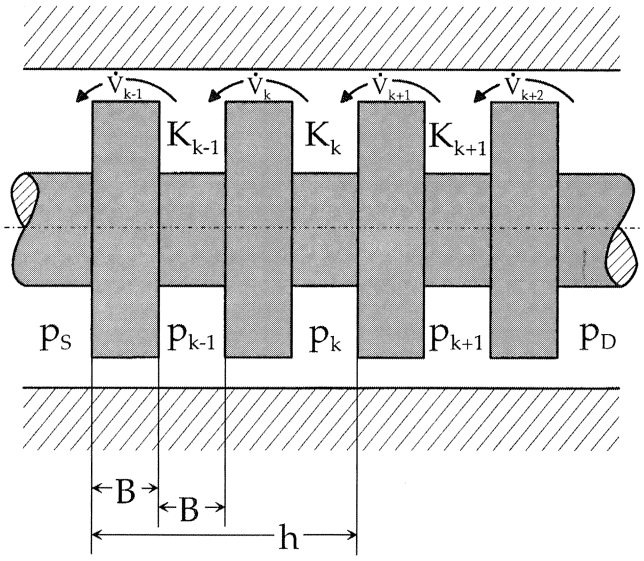

Figure 10. Circular Disc Model for Double-Thread Layout.

The pump's discharge procedure as explained depends on time or speed because the individual pump chambers are only involved during their lifetime (speed in rpm):

$$\tau_K = \frac{60}{n \cdot G} \tag{16}$$

Modeling the Leak Flow Through the Circumferential and Radial Clearances

In this case, the leak flows remain within the relevant screw and can be therefore treated related to the individual screw only (Figure 11(a)). As indicated it must be distinguished between two (2+2) and three (3+2) chamber engagement (Figure 11(a), left and right). Please note the nomenclature with two examples:

- Through the circumferential clearance, CC_{D2}, flows the leak loss from the discharge (D) to the second chamber (2) with the driving pressure differential, $\Delta p_{CCD2} = p_D - p_2$.
- Through the radial clearance, RC_{2S}, flows the leak loss from chamber 2 to the suction (S) chamber with the driving pressure differential, $\Delta p_{RC2S} = p_2 - p_S$.

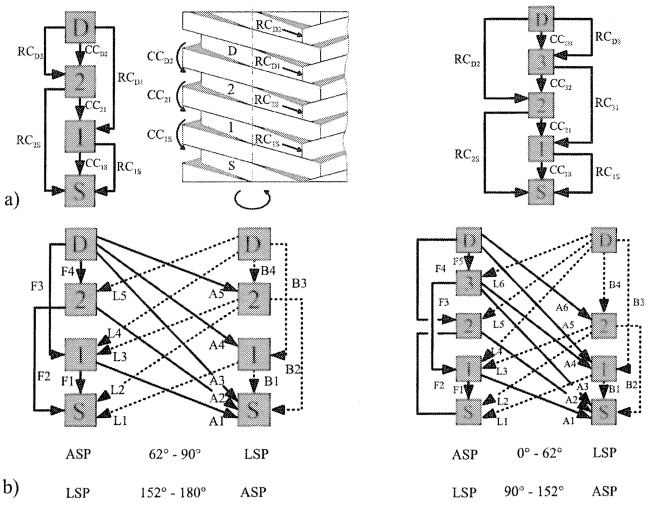

Figure 11. Modeling the Real Pump. (Left: Two chamber layout; Right: Three chamber layout; (a) Circumferential and Radial clearance; (b) Flank clearance; ASP: Driving screw; LSP: Driven screw)

Modeling the Leak Flow Through the Flank Clearances

In this case, the screw package sees (Figure 11(b)) transverse leak flows and again two (2+2) and three (3+2) chamber engagement must be distinguished (Figure 11(b), left and right). It can be understood that leak flows through flank clearances (various types A, B, F, L) interact within (ASP driving screw, LSP driven screw) and between the screw. (For further details, refer to Körner, 1998.)

Please note, for example, the total leak flow into the suction (inlet) chamber of both screws through the various flank clearances involved:

$$V_{LF3ch} = F1+F2+L1+L2+B1+B2+A1+A2+A3 \tag{17}$$

Evaluation of the Total Leak Flow

The leak flows for the two (2+2) and three (3+2) chamber operations have to be totaled by evaluating and weighting the different contributions:

$$\dot{V} = \delta \cdot \dot{V}_{L3ch} + (1-\delta)\dot{V}_{L2ch} \tag{18}$$

$$\dot{V}_{L3ch} = 4 \cdot \dot{V}_{L,CC+RC,3ch} + 2 \cdot \dot{V}_{L,FC3ch} \tag{18a}$$

$$\dot{V}_{L2ch} = 4 \cdot \dot{V}_{L,CC+RC,2ch} + 2 \cdot \dot{V}_{L,FC2ch} \tag{18b}$$

Thermodynamics of the Gas Compression

The rapid gas compression in the chambers during their short lifetime by the backflow through the clearances will follow a polytropic change of state. Due to the intensive direct turbulent heat exchange, the real change of thermodynamic state will tend to be isothermal. The specific heat capacity and the mass of the liquid fraction are extremely high compared with that of the gas.

The performance of twin-screw pumps becomes rather inefficient for gas fractions larger than 95 percent and breakdown of the pump function as well as dry-running conditions should be

avoided. Installing suitable control and liquid injection devices are recommended to protect the pumping system (Wincek and Moser, 1999; NN Westinghouse Electric Co., 1999).

The pump modeling has been approximated by isothermal change of thermodynamic state during compression.

The Computer Program MEFAP

The new MEFAP computer program presented here (Körner, 1998) is based on an earlier version (Vetter and Wincek, 1993b). It represents the software tool to predict multiphase twin-screw pump performance based on the pump model explained in the previous section (Vetter and Körner, 1998).

- *Input data*—Geometry of the screws, dimensions of the clearances, surface roughness, liquid/gas data, suction/discharge pressure, gas fraction on suction, speed of the pump
- *Output data*—Pump capacity, total leak flow, leak flows through defined clearances, pressure distribution

The actual version of this program is suitable for a limited number of twin-screw pump layouts, but can be easily adapted to other requirements.

Please note: This computer code uses subroutines for the determination of the density and viscosity of the fluid-mixture, the deflection of the spindle shafts due to the bending load, and the momentary pump performance during the time periods of different pump chamber engagement modes.

Experimental Phenomenology

Three commercial pumps have been experimentally investigated in total (Wincek, 1992; Vetter and Wincek, 1993b; Körner, 1998). This paper mainly provides results of the last campaign comprising the full range of the gas fractions (up to 98 percent) and the complete data set about performance and pressure distribution along the screws.

The data of the twin-screw test pump are provided by Table 3 and Figure 12. The test rig was suitable for two-phase water/air-mixtures. For the large gas void fractions (more than 90 percent), the water was injected by a reciprocating metering pump system into the gas stream in order to obtain good stability and accuracy. The definition of the gas void fraction (related to suction conditions) is:

$$\alpha = \frac{\dot{V}_g}{\dot{V}_{liq} + \dot{V}_g} \tag{19}$$

The tests were normally operated from ambient (1 bar) suction to a maximum 20 bar discharge pressure. The pump was instrumented with a number of sensors (p_1 to p_7) for measuring the pressure distribution along the screws and their deflection due to bending forces (w_1, w_2, in perpendicular axis). The attempt to measure the fluid conditions (liquid fraction in the gas) in the circumferential clearances was not successful (f_1 to f_3) (Körner, 1998). All data reported here are related to a speed of 2800 rpm only, close to the maximum. The performance in detail depends on the speed. Basically, the capacity is linear but not proportional with speed because the capacity/speed-correlation (at p = constant) exhibits a characteristic offset due to the internal leak losses through the clearances (Vetter, 1998).

Volume Flow and Efficiency

The total flow rate, $\dot{V}$, of the two-phase mixture exhibits comparably (Figure 13) to what has been reported earlier (Neumann, 1992; Christiansen, 1986; Vetter and Wincek, 1993b). Starting from pure liquid (α = 0 percent), the flow rate, $\dot{V}$, grows with increasing gas void fraction (α < 50 percent), and then decreases more and more (α > 50 percent), until the pumping action finally breaks down (close to α = 96 percent, all data are related to Δ_p = 15 bar).

Table 3. Test Pump Data.

External diameter of the screw D	100 mm
Internal diameter of the screw d	70 mm
Pitch of the screw h	50 mm
Length of the screw l_s	120 mm
Width of the screw profile B	12.5 mm
Width of the chamber	12.5 mm
Number of screws S	2
Number of threads G	2
Number of chambers (stages) k	3.347
Mean surface roughness R_t	4 µm
Average width of circumferential clearance s_{CC}	187.5 µm
Average width of radial clearance s_{RC}	105 µm
Average width of flank clearance s_{FC}	75 µm
Displacement volume per revolutio V_U	$3.60 \cdot 10^{-4}$ m^3
Volume flow $\dot{V}$	630 l/min
Pressure differential Δp	20 bar
Nominal speed n	3000 U/min

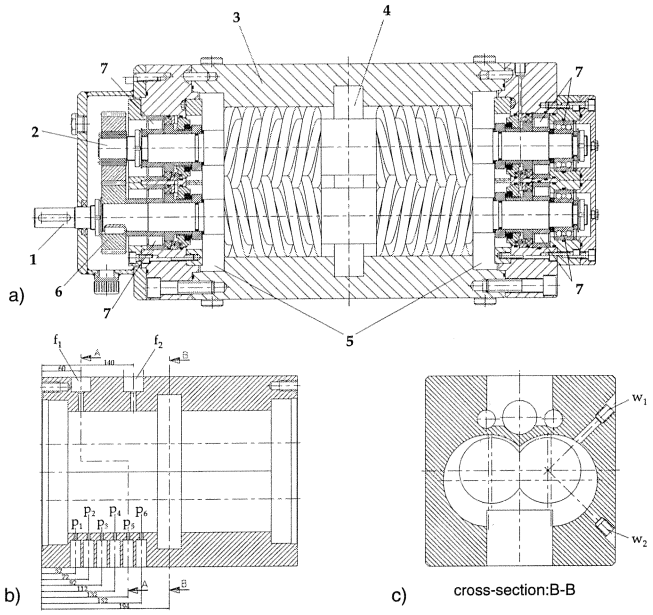

Figure 12. Test Pump. ((a) Cross section: 1. Driving shaft (ASP), 2. Driven shaft (LSP), 3. Pump housing, 4. Discharge, 5. Suction, 6. Gear, 7. Bearing; (b) Locations for sensors ($P_1 \div P_6$ pressure; F_1, F_2 humidity); (c) Locations for sensors (w_1, w_2 shaft deflection))

The characteristics as explained can be understood if the pressure distributions along the screws are considered (refer to next section). Please note: the pumps size and speed affects the performance observed in details but not in general.

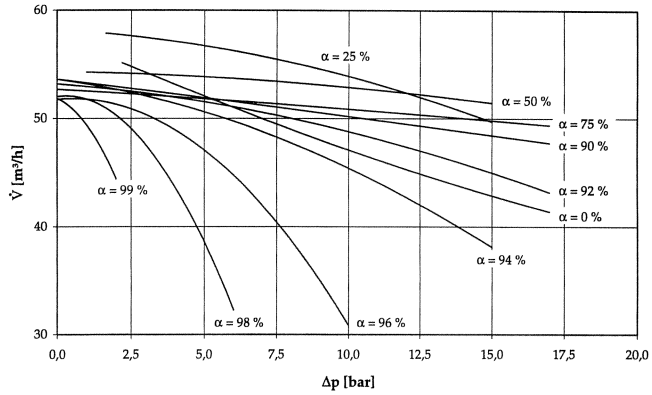

Figure 13. Volume Flow at Various Gas Void Fractions (2900 RPM).

Concerning the power input into the pump, it should be noted that the torque, T, required at the pump coupling shaft stays constant with the gas void fraction, α, and correlates linearly with the pressure differential, Δp. A very important term is the volumetric efficiency representing the ratio between the real two-phase suction flow, $\dot{V}$, and the geometrical suction flow, $\dot{V}_{geo}$.

$$\eta_{vol} = \frac{\dot{V}}{\dot{V}_{geo}} \tag{20}$$

Figure 14(a) clearly shows the favorable performance of twin-screw pumps for two-phase operation. Up to more than 95 percent gas void fraction, the capacity of the pump stays very stiff with respect to the pressure differential, demonstrating continuous and stable pumping action at varying gas fractions. These results with the small test pumps perform better still for larger units.

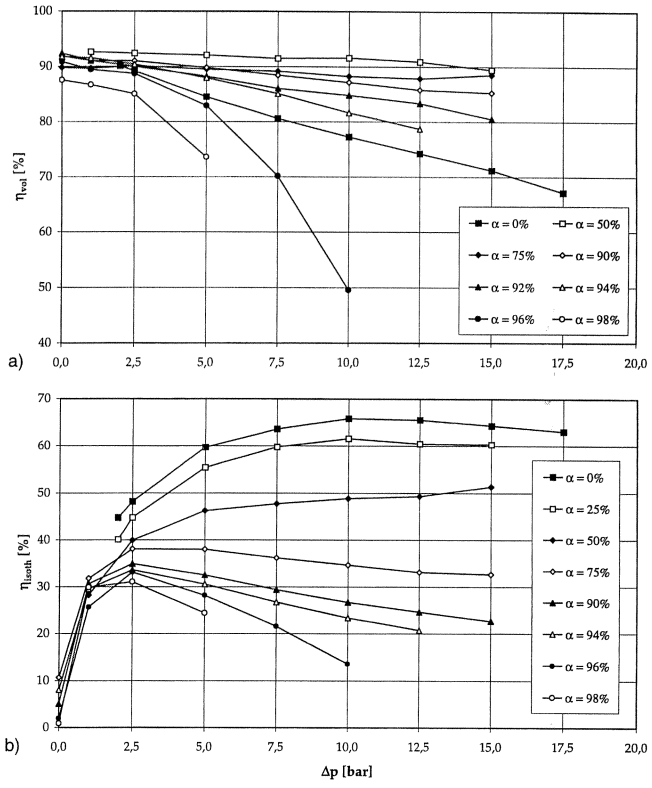

Figure 14. Volumetric (a) and Isothermal Efficiency (b) (1900 RPM) at Different Gas Void Fractions.

Figure 14(b) further shows the isothermal efficiency, η_{isoth}, representing the ratio between the totaled energy input into the fluid mixture (isothermal liquid and gas compression) and the real power consumption (torque, T, multiplied with angular velocity, ω).

$$\eta_{isoth} = \frac{\dot{V}_{liq}\cdot\Delta p + p_S\cdot\dot{V}_g \ln(p_D/p_S)}{\omega\cdot T} \tag{21}$$

Due to the characteristic mode of the gas compression generated by the leak flows into the pump chambers, the isothermal efficiency decreases greatly with a growing gas void fraction.

The twin-screw pump is a good two-phase pump, but not an ideal gas compressor.

Pressure Distribution along the Screws

Evaluating the mean pressure signals of the sensors distributed along the screw provides evidence about the changing pressure gradients with the gas void fraction (Figure 15(a), (b), (c)).

- *$0 < \alpha < 80$ percent*—Starting with linear pressure distribution for pure liquid flow, the pressure gradient becomes steeper, ending with the last chamber carrying nearly the full pressure differential. Obviously the clearances stay filled with liquid leak flow in order to achieve the high compression in the last chamber.

- *$80 < \alpha < 100$ percent*—With further growing gas void fraction, the pressure gradient moves backward again and turns more and more to linear, indicating the fluid in the screw spaces behaves homogenous (foam) like the liquid. The examples with very large gas void fractions (Figure 15(b), Δp = 10 bar, α = 96 percent; Figure 15(c), Δp = 5 bar, α = 98 percent) demonstrate that the pressure distributions for pure liquid (α = 0) and those close to pure gas finally coincide.

In order to point out clearly the difference between the two groups of behavior considered above, Figure 16 demonstrates the situation at the sensor, p_5 (located at 92 mm length of the screw): The pressure sensors as installed during the rotation of the screw alternatingly "see" a chamber or the circumferential clearance (width of the flight) or a transition range in between (refer to notes in Figure 16).

- *α = 75 percent (Δp = 15 bar, 2900 rpm, Figure 16(a))*—The largest part of the compression is performed within the third chamber (refer to 80 to 180 degrees, minimum 3 bar, maximum 21 bar). The pressure is increasing first slowly (leak flow) and then rapidly (refer to 145 to 180 degrees of φ) opening to the discharge and reflux from there (refer to coinciding pressure decrease, p_6).

The first peak (above the mean discharge pressure) obviously is a result of the shock-like reflux. The second one can be related to the rapid discharge wave following. The other locations and chambers (sensors p_1 to p_4) do not participate much (except p_4 slightly, second chamber) in the compression.

- *α = 90 percent (Δp = 15 bar, 2900 rpm, Figure 16(b))*—In contrary to the case explained before, in this situation, the pressure distribution has already moved slightly back toward linearity. The pressure fluctuations yield rather similarly as shown in Figure 16(a). Refraining from detailed explanations, here it can be seen clearly that now the other chambers are starting to contribute (refer to p_4) more and more to the fluid compression. The clearances see more and more liquid/gas-mixtures. This process continues (Figure 16(c)) with a further increasing gas void fraction.

Polytropic Exponent

The experimental data—inlet/outlet temperature measured separately for liquid and gas—clearly demonstrate that the compression process is really close to the isothermal up to gas void fractions of around 96 percent. The polytropic exponent, N, (Figure 17) is evaluated as follows (T_D/T_S and p_D/p_S: temperature/pressure ratio):

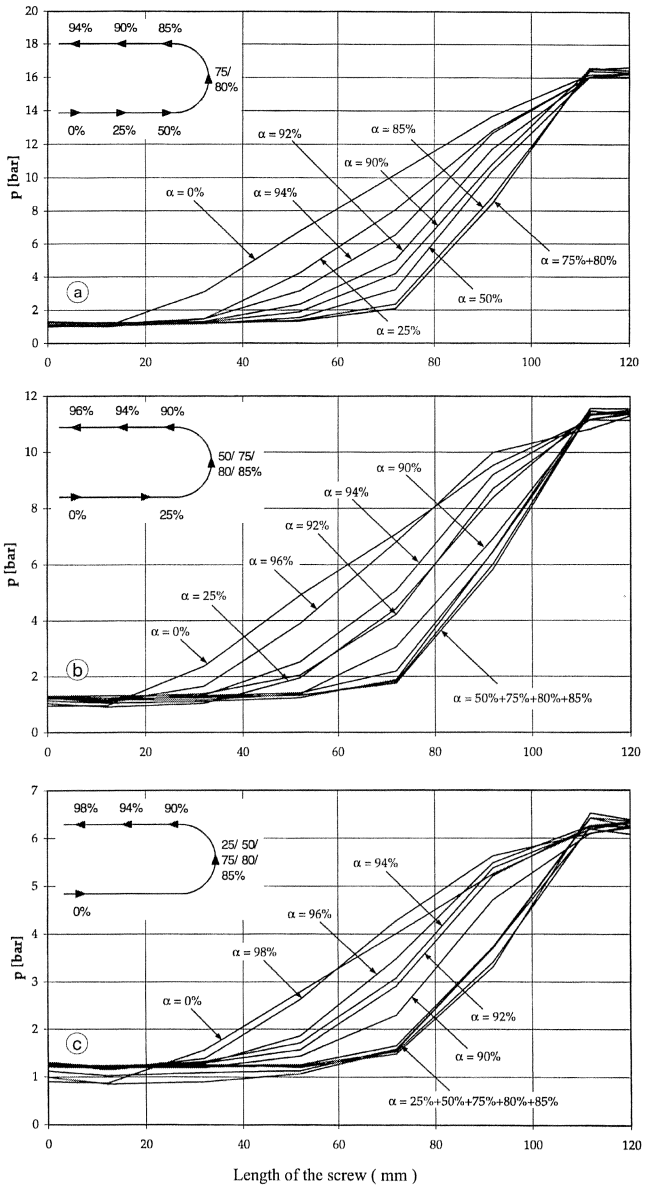

Figure 15. Pressure Distribution along the Screw (2900 RPM). ((a) Δp = 15 bar; (b) 10 bar; (c) 5 bar)

$$N = \left[1 - \frac{\ln(T_D/T_S)}{\ln(p_D/p_S)}\right]^{-1} \qquad (22)$$

The study of the parameter influences shows that, with growing compression ratios and gas void fractions, the deviations from the isothermal conditions will increase. Methods to approximately predict these effects are avoidable (Körner, 1998). It should be noted that the temperature developed is not only determined by the compression heat, but also by the dissipation of energy by the leak losses.

Experimental Verification of the Computational Predictions

The pump model implemented into the computer program discussed evidently meets the real pump performance satisfactorily well (Figure 18). The deviations at the high level of the gas void fractions must be related to the obvious uncertainties of the assumptions on which the model is based, with respect to the fluid state within the clearances (more verifications for larger twin-screw pumps in field service (refer to Wincek and Moser, 1999)).

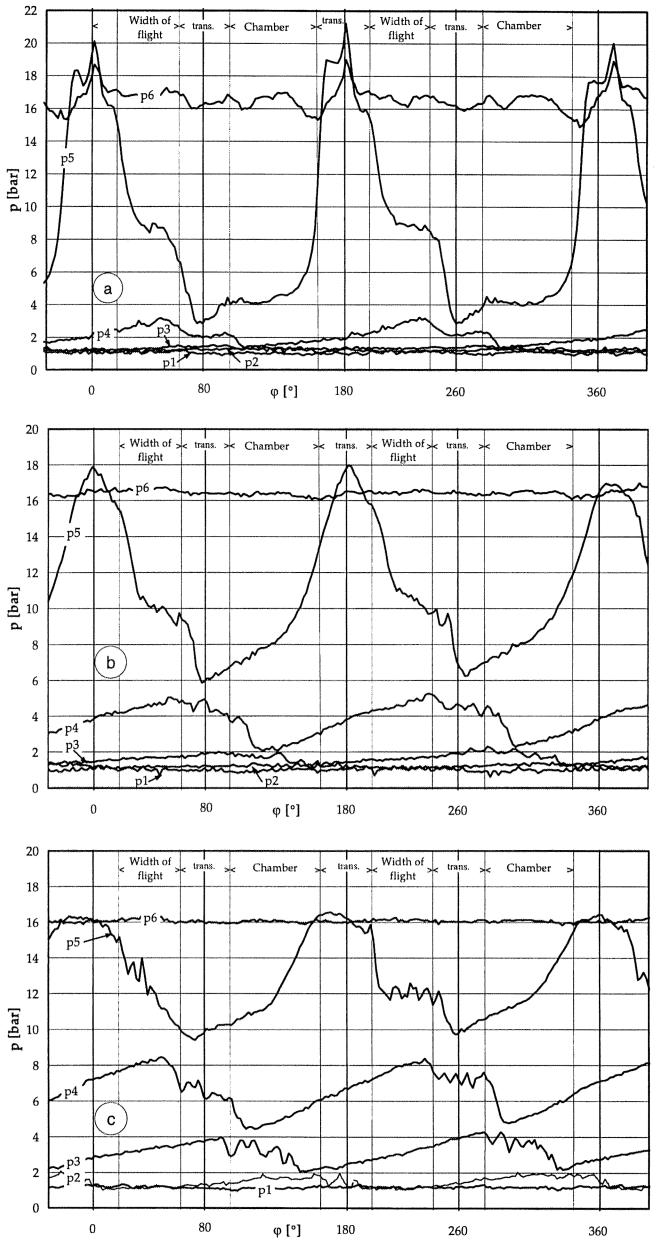

Figure 16. Pressure Fluctuations (p(φ)) at the Pressure Sensor p_5 (2900 RPM, Δp = 15 Bar, φ Angle of Rotation). ((a) α = 0.75; (b) α = 0.90; (c) α = 0.94.)

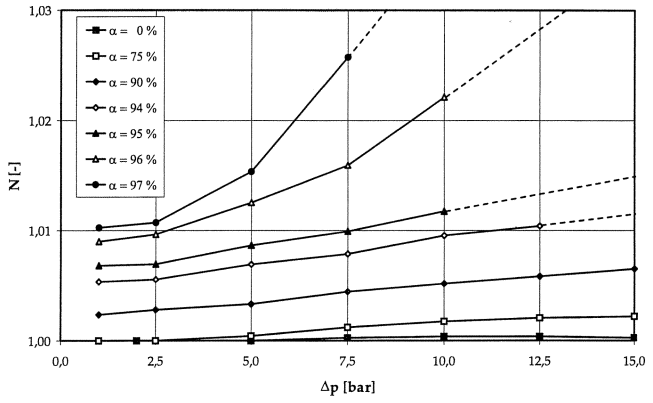

Figure 17. Polytropic Exponent (Test Pumps).

Furthermore an impressive proof for the acceptable modeling quality is given by the fact that the pressure distributions along the screws (Figure 19) are predicted pretty well by the computation.

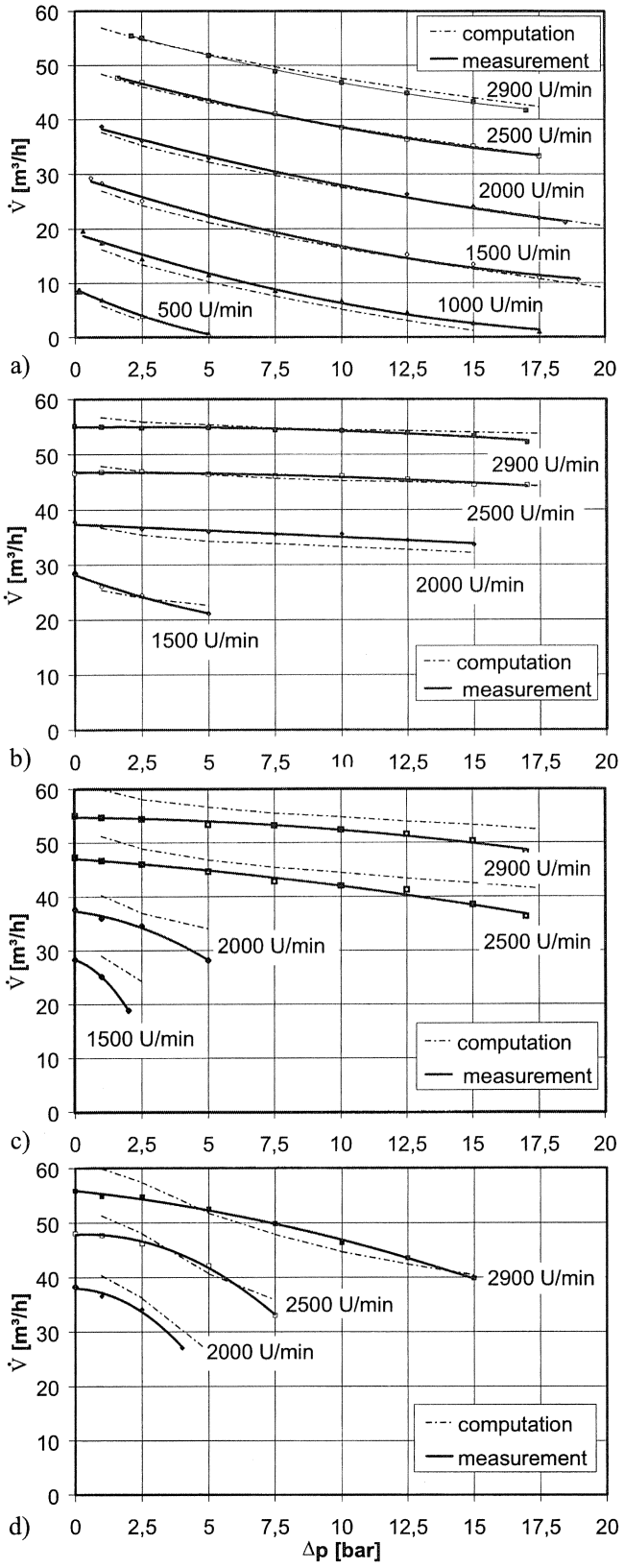

Figure 18. Pump Performance for Different Gas Void Fractions and Pump Speeds—Measurement and Computation. ((a) α = 0; (b) α = 0.8; (c) α = 0.9; (d) α = 0.94)

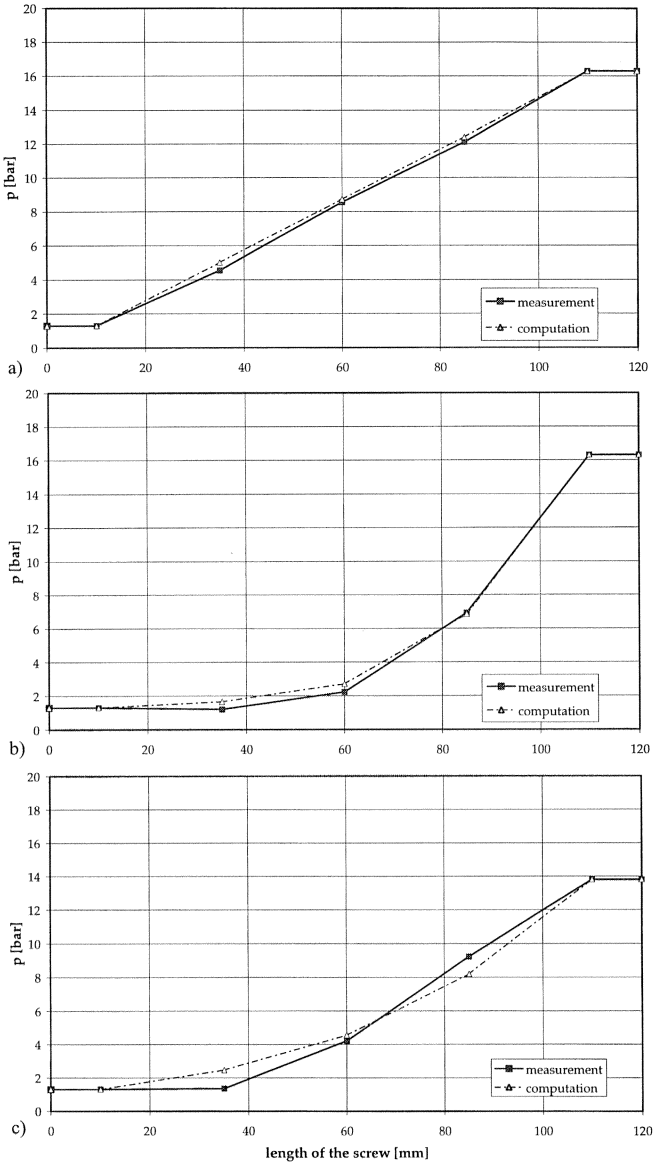

Figure 19. Pressure Distribution along the Screw—Computation and Measurement. ((a) α = 0; (b) α = 0.9; (c) α = 0.94)

HYDROABRASIVE WEAR IN TWIN-SCREW PUMPS

As the previous sections point out, a suitable configuration of the sealing clearances is very important to avoid malfunction of the twin-screw pump. In the field of multiphase pumping, it is necessary to ensure that the dimensions of the clearances stay intact under hydroabrasive wear attack for the whole life-cycle of the pump.

The only means to completely avoid hydroabrasive wear in multiphase pumps would be a complete solid/liquid separation device at the suction side of the pump. This however is not a realistic approach due to economic and operational reasons.

The particle contamination of the fluid mixture as it is discharged from the well varies greatly in concentration and the minerals involved. Typically, the concentration stays below one percent and the minerals contain a large percentage of types with lower hardness (e.g., feldspar: 600 to 700 HV, limestone: 200 to 300 HV) and only a small fraction of highly abrasive silica sands (around 1100 HV).

Before installing a pump, the abrasive potential of the fluid must be determined and the pump engineer should find solutions for the proper protection of the engine against wear attack.

The following section presents some guidelines for that task.

Tribological Analysis and Wear Simulation

In the introductory section, the existing wear mechanisms (Figure 4) have already been characterized. As the circumferential clearances show by far the largest meshing ratio (Figure 3, bottom), further report will be concentrated on that subject only.

The two important wear mechanisms in the circumferential clearances are jet wear (particles smaller than the clearance width) and sliding wear (particle size in the magnitude of the clearance width). Vetter and Kießling (Vetter and Kießling, 1996; Kießling, 1994) have studied the hydroabrasive wear in annular clearances (inner part rotating) and found enormous difference in the linear wear rates under jet and sliding wear conditions, illustrated by the SEM picture (Figure 20).

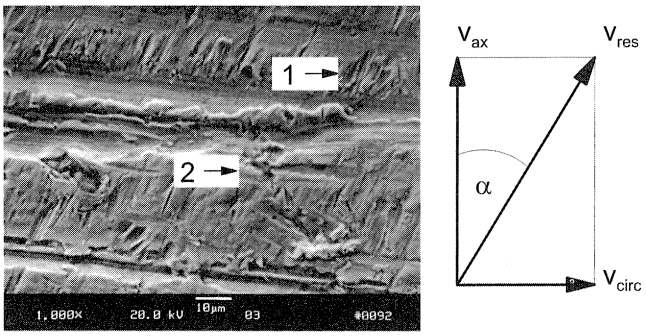

Figure 20. Jet (1) and Sliding (2) Wear Traces (SEM). (Right: Velocity diagram oriented like the SEM photo)

In this case, the particle collective included particle sizes of the same magnitude as the width of the clearance (d_{pm} = 186 µm, s_{CC} = 200 µm). Jet wear traces (Figure 20, item 1) can be seen in the resulting direction of the flow, dissected circumferentially by the far larger sliding wear traces, characterized by deep grooves.

Please note: In twin-screw pumps, the most effective potential of hydroabrasive wear is located at the circumferential clearance and caused by particle fractions with a magnitude comparable to the width of the clearance. If any separating devices should ever be applied, removing these dangerous particle sizes should be attempted.

Generally there are two different approaches to analyze the wear process of screw pumps:

- On the one hand, wear investigations can be made by means of field tests with the pump. In this way, the real wear effects on the pump can be evaluated. This approach however turns out to be expensive and time consuming, and moreover delivers wear data only for the individual tested pump—the transfer to other sizes of pumps or even functionally different pumps is normally impossible.

- On the other hand, the wear testing can be done with tribometers—technical devices that allow simulation of the wear process of the pump in a relatively simple test rig at much lower costs. Thereby it is possible to conduct test series with a larger number of materials. The limitation of the tribometric method however is given by the quality of the achievable result: Generally, a *quantitative analysis* of the pump is quite complex and can only be done by means of a specialized tribometer; but often the *qualitative analysis* of a tribometric system under the variation of certain parameters already gives the desired results to improve the life-cycle of a pumping system.

A rather perfect simulation of wear in the circumferential clearances of screw pumps can be achieved by the rotary clearance tribometer (RCT) (Figure 21). Its functional principle is based on the combination of a static outer cylindrical housing and a rotating inner cylinder. The two cylinders can be manufactured from various material combinations and a characteristic particle suspension can be circulated.

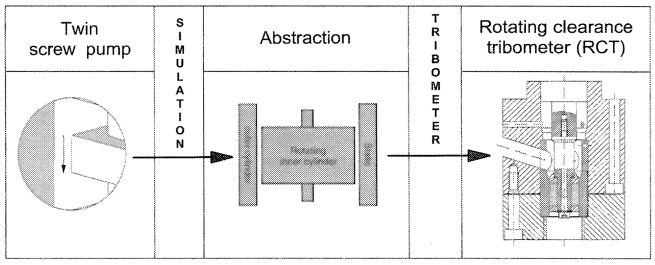

Figure 21. Simulation with the Rotating Clearance Tribometer.

The tribometer is integrated into a test loop for the suspension, comprising a reservoir with a stirring device, a circulation pump, and a flowmeter.

In the case of the multiphase twin-screw pump studies, the tribometer was used to determine the protective potential of different hard coatings.

The RC tribometer simulates the clearance flow quite precisely because it can operate at the same or similar circumferential and resultant velocity. The relation between the width of the clearance and the size of the particle collective can be adjusted close to reality as well as the geometry involved in general (very small width of the clearance compared with the diameter of the cylinder).

The particle concentration influences the resulting wear rates linearly. Therefore a time compression of the tests can be achieved by simply increasing the concentration of solids in the suspension. Another time compression was implemented by testing with a pure silica sand suspension with the particles involved exhibiting the highest hardness among the minerals present in oil/gas wells.

Parameter Influences on Hydroabrasive Wear in Clearances

In order to understand the potential of the various parameters and to design pumps in a wear protective way, the main correlations are quickly explained. Table 4 gives an overview of relevant wear parameters classified by flow, abrasive particles, geometry, and pump material parameters (Vetter and Kießling, 1996; Kießling, 1994).

Table 4. Wear Parameters.

	parameter	linear wear rate	
Fluid	velocity		
	screw, rotating cylinder	$W_l \sim v_{res}^{2.93} = \sqrt{v_{ax}^2 + v_{circ}^2}^{2.93}$	(23)
	housing, static cylinder	$W_l \sim v_{ax}^3$	(24)
Particles	concentration	$W_l \sim c_P$	(25)
	size	$W_l \sim d_{Pm}$	(26)
Geometry	meshing ratio	$W_l \sim M_R$	(27)
	clearance width	$W_l = (0.65...1.0)\ s^{-(1.1...1.4)} \cdot \dot{V}$	(28)
Material	hardness	$W_l = f(R_h)$	(29)

Flow Parameters

The main flow parameter affecting pump wear is the velocity of the clearance flow. The wear of the screw tips (RCT: inner cylinder) is influenced by the resulting speed composed of axial and circumferential velocity, the wear of the housing (RCT: outer cylinder) by the mere axial velocity. In both cases, a power law with an exponent of 2.93 (screw) or 3 (housing) gives a good correlation between flow velocity and wear losses (linear wear rate, W_l).

Particle Properties

In good approximation, the wear losses are proportional to both particle concentration and mean particle diameter, as long as the magnitude of the particles is small compared with the width of the clearances and the tribosystem is in the jet wear regime.

As soon as the magnitude reaches the width of the clearances, jet wear is superimposed by sliding wear with an increase of wear losses by nearly a factor of 10.

Quantitative predictions are not possible as the wear depends on the magnitude distribution of the particles. In this case, RCT tests represent a good tool to obtain data about the hydroabrasive potential of the tribosystem.

Pump Geometry

The wear losses increase proportionally with the meshing ratio. At a constant speed of the flow, the linear wear rate initially decreases substantially as the width of the clearance increases, since for wider clearances the probability of a particle to hit a wall is less. After a minimum, the linear wear rate rises for even wider clearances by a small amount. For constant velocity of flow, the volume flow rises, however, according to the increase in the cross sectional area, admitting more wear particles into the gap. Both effects are superimposed and described by the correlation given in Table 4.

Material Hardness

The hardness ratio, R_h, between the attacking particles (HV_P) and wearing material surfaces (HV_M) is an outstanding parameter for hydroabrasive wear in general. A drastic decrease of wear is achieved by the transition from the low wear level ($R_h < 1$) to the high wear level ($R_h > 1$), as shown in Figure 22. The wear rates are reduced by a factor of 100 or more.

Predictions of the correlation of the linear wear rate with the hardness ratio can be evaluated by tests with the RC tribometer.

Concerning the twin-screw pump, most of the wear parameters are fixed by design (e.g., width of the clearances) or by the operational parameters (e.g., speed)—the main potential for wear reduction is given by the choice of material for the screws and the housing at the location mainly exposed to the wear attack. Earlier investigations (Vetter, et al., 1996) show the material hardness of the conveying elements being the main parameter to concentrate on.

Furthermore, it is a good step to reduce flow velocity in the clearances by installing a screw package with an adequate number of stages.

Material Selection

Due to the bending load involved, the material for the screws should exhibit a tough, ductile core with a relatively thin hard surface layer at the locations submitted to highest wear attack.

A comprehensive study (Höppel, et al., 1999) during an inter-disciplinary approach yielded the following suitable material treatments:

- The modification of the surface layer by thermal hardening or thermochemical means by nitriding or boronizing
- The application of coatings mainly by flame, plasma, and detonation spraying

This selection takes care of the stringent need for a very hard, well adhering, and sufficiently thick coating layer.

As within the particle contamination, silica sand fractions with a Vickers hardness of more than 1100 have to be expected, the required hardness should exhibit even harder (HV 1200 to 1500). The bonding should be of utmost quality against bending and shearing stresses (from friction).

Furthermore, the coating material should offer enough toughness of the matrix to avoid brittle rupture and exhibit a

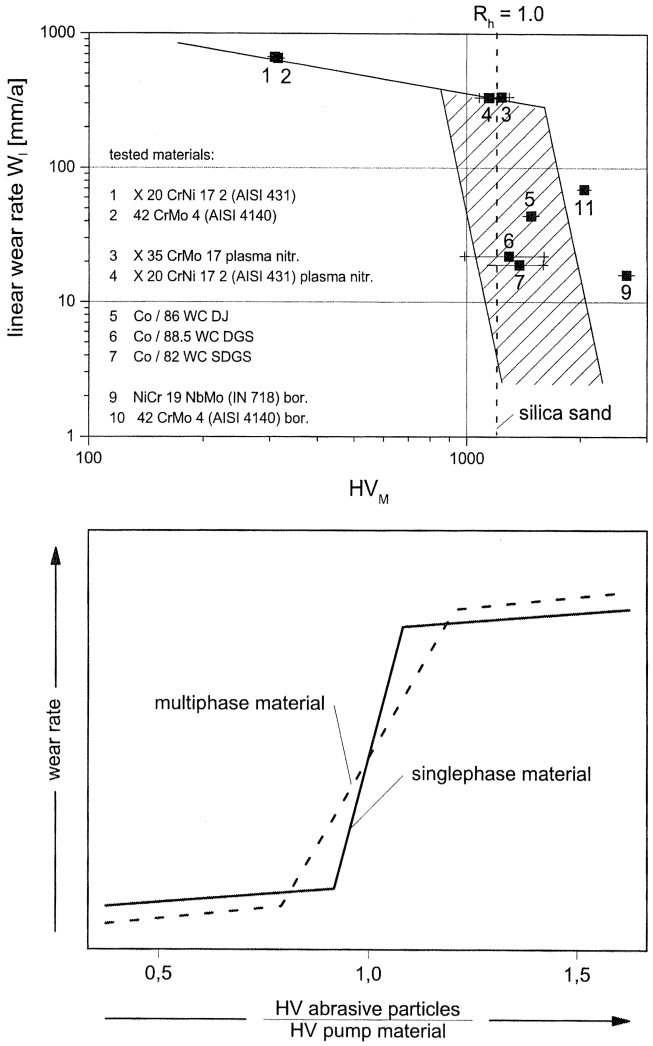

Figure 22. Influence of the Hardness Ratio R_h.

thickness of at least 0.5 to 1 mm to endure the local indentation and ploughing stresses by the particle attack without being penetrated. This is the reason why thin coatings (chemical vapor deposition (CVD), physical vapor deposition (PVD)) have turned out to be not suitable at all under hydroabrasive wear attack.

Table 5 shows an extract from a larger number of materials (combinations, treatments, coatings) consisting of monophase (e.g., the heat treated and nitrided types of steels and the steels onto which a coating was applied by boronizing) and multiphase (e.g., coatings on steel substrates containing tungsten carbide particles in different Co/Cr to matrices) types. The materials listed in Table 5 represent a wide range of hardness from around 300 to 2600 HV.

The hardness values depend on the load applied: The homogenous heat-treated steels yield reproducible results, the nitrided types exhibit load dependency of HV due to the relatively thin nitrided layer (around 200 µm). The multiphase types, if HV-tested at a very low load, show large fluctuations as regions of very different hardness are involved. The boronized surfaces yield reproducible HV results, again as they exhibit homogeneousness.

Tests with the RC tribometer (Figure 23) demonstrate an extreme dependency of the linear wear rate on the hardness ratio, R_h.

All tests have been performed with silica sand suspensions with a choice of the mean particle diameter, in a way that jet wear as well as sliding wear conditions could be achieved alternatively.

The linear wear rate under sliding wear conditions yields around a factor of 10 higher. It should be noted that the gradient is more or

Table 5. Selection of Materials for Multiphase Screw Pumps. (WC: Tungsten carbide; SDGS: Super detonation gun spraying; DGS: Detonation gun spraying; DJ: Diamond Jet™; ●: Field test)

name	Treatment	coating method / composition fracture WC / particle size	HV02	HV(3)	Testing
X35 CrMo 17 ● WNr. 1.4122 similar S 42080	heat treated	-	-	303 ± 3	RCT Field
X20 CrNi 17 2 WNr. 1.4057 AISI 431	heat treated	-	-	315 ± 4	RCT
42 CrMo 4 WNr. 1.7225 AISI 4140	heat treated	-	-	309 ± 5	RCT
X35 CrMo 17 ● WNr. 1.4122 similar S 42080	plasma nitrided	-	1239 ± 58	(932 ± 67)	RCT Field
X20 CrNi 17 2 WNr. 1.4057 AISI 431	plasma nitrided	-	1144 ± 64	(876 ± 73)	RCT
Co / 86 WC DJ X20 CrNi 17 2	Coated	DJ / 86 WC, 10 Co, 4 Cr 55.3 vol.-%WC / 0.34 µm	1482 ± 32	-	RCT
Co / 88.5 WC DGS ● X20 CrNi 17 2	Coated	DGS / 88.5 WC, 8.5 Co, 3 Cr 19.5 vol.-%WC / 0.70 µm	1295 ± 308	-	RCT Field
Co / 82 WC SDGS X20 CrNi 17 2	Coated	SDGS / 86 WC, 10 Co, 4 Cr 55,3 vol.-%WC / 0.61 µm	1379 ± 216	-	RCT
42 CrMo 4 WNr. 1.7225 AISI 4140	boronized 900°	-	2049 ± 28	-	RCT
X35 CrMo 17 ● WNr.1.4122 similar S 42080	boronized 900°	-	> 2000	-	Field
NiCr 19 NbMo IN 718	boronized 900°	-	2648 ± 56	-	RCT

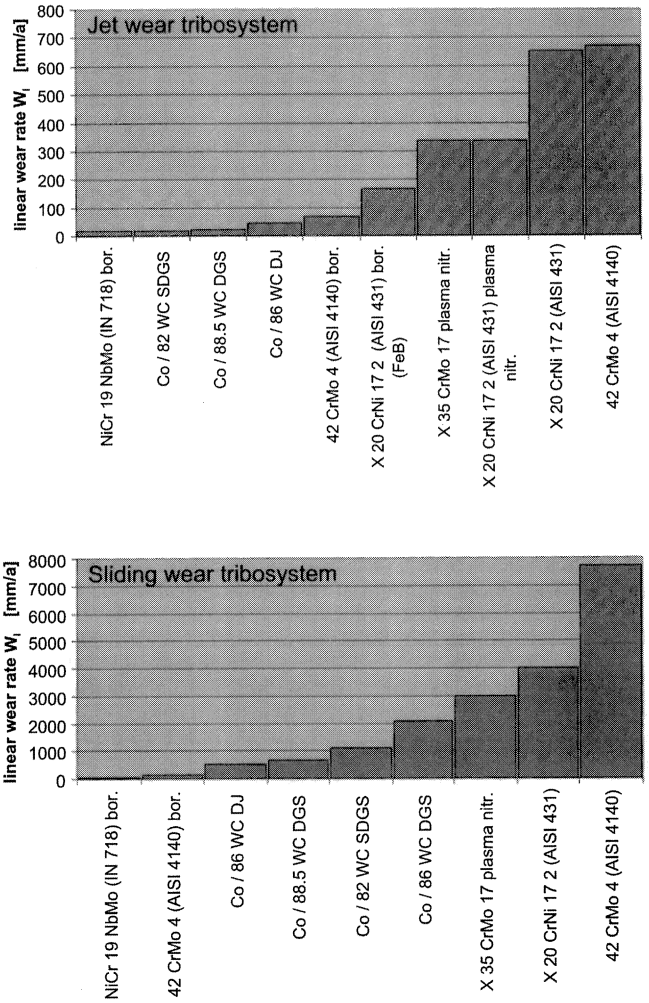

Figure 23. RCT Linear Wear Rates for Jet and Sliding Wear (v_{ax} = 25 m/s).

less sharp for single and multiphase materials (Figure 22) (Zum Gahr, 1990). The very complex microstructure based effects that are especially involved when considering the protective potential of hard particles will not be treated here in detail. A very good overview is given in (Höppel, 1997).

The same applies for the choice of the coating design with respect to the size of the hard particles, their concentration, and the bonding matrix. Also, the corrosion resistance of the material is an important factor.

It should be pointed out clearly that the RC tribometer tests provide a good prediction for the wear resistance of materials. For practical applications and quantitative predictions, the particle suspension should well represent the conditions of the real case.

Please note further: Wear protecting coatings must be selected not only with respect to the wear reduction, but also with respect to reliable production and long-term bonding quality (no delamination should occur!).

Pump Wear and Testing

The "field tests" were performed with the test pump (Figure 12, Table 3) operating with a water/silica sand suspension (Table 6), searching answers for the following questions:

- Are data concerning the relative suitability of materials transferable between RCT tests and field tests for the twin-screw pump?
- How is the local wear phenomenology in twin-screw pumps exhibited?

Table 6. Data for Pump Wear Testing.

Suspension	
Abrasive particles	Silica sand
Particle distribution	40 – 150 µm
Mean particle diameter	83 µm
Concentration of solids	2 weight-%
Fluid	Tap water
Geometry	
Average width of circumferential clearance s_{CC}	187.5 µm
Average width of radial clearance s_{RC}	105 µm
Average width of flank clearance s_{FC}	75 µm
Operation	
Type of tribosystem	Jet wear
Pressure differential Δp	14 bar
Nominal speed n	2000 U/min
Axial velocity	21 m/s
Tangential velocity	10.5 m/s

Method of Relative Suitability

Four material combinations (screw tips, bushings) have been selected (refer to Table 5, ●) to learn whether the RCT and the field test results yield similarly.

The pump features were operated with the same parameters (speed, pressure differential, silica sand suspension) as the RCT, until the capacity of the pump had decreased to around 25 percent of the initial value due to the increased width of the clearances.

The time to arrive at the end of the pump's operational period was used as the measured value for the materials' wear resistance or wear rate.

The result (Figure 24) is quite impressive demonstrating that the relative suitability of the materials predicted by the RCT testing is more or less identical with that of the pump (field) test.

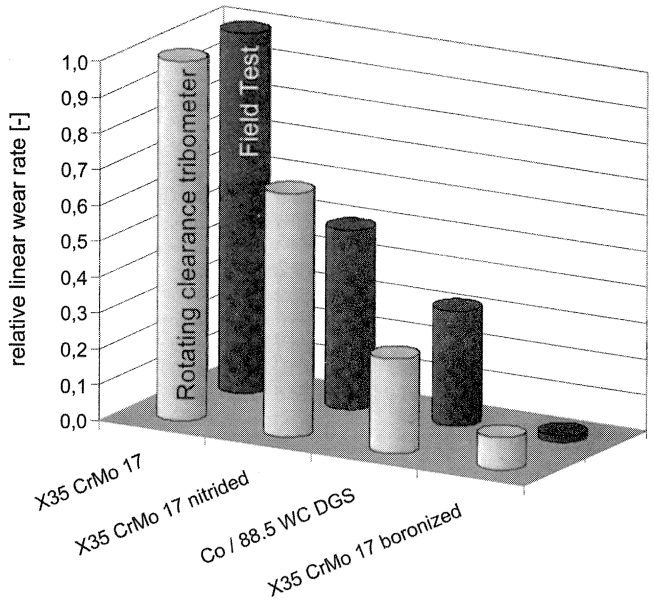

Figure 24. Relative Suitability of Materials—Field (Pump) Test/RC Tribometer.

This again confirms how efficient the tribometer tool is to improve the pump's wear resistance and extending its life period.

Please note: The coating technology for the screws requires much experience and a number of development steps in order to achieve good operational results. The coating layers should be thick enough and protect the edges at the screw's tip too. The selection of the coating type should take care of the material properties as well as the reliable reproducible quality of the production process.

Phenomenology of Pump Wear

In order to provide a close look into the wear effects, 3D measurements of the screw package as well as the bushing have been performed. The results are explained for the following material combination:

- Screw: X35 CrMo 17, WNr. 1.4122, similar S 42080, plasma nitrided
- Bushing: X35 CrMo 17, WNr. 1.4122, similar S 42080

The phenomenology of the local wear rates demonstrates expected as well as unexpected results:

- As expected, the wear rates of flank and radial clearances yield much smaller than those of the circumferential clearances (screw tip/bushing).
- The wear pattern of the circumferential clearances (Figure 25) unexpectedly does not exhibit a constant in the axial direction of the screw package, but decreasing. This behavior is the same for all the other material combinations tested with the RCT.

For the example observed, the wear at the housing is slightly larger than that at the screw tips, although the meshing ratio at the housing is smaller. The reason obviously is that the bushing is not nitrided.

- The edge of the screw tip directed toward the discharge side of the pump is showing excessive wear trace (Figure 26(a)), obviously effected by jet wear from the leak flow through the chamber (Figure 26(b)).

More information about the wear phenomenology is found in Schmidt (1999).

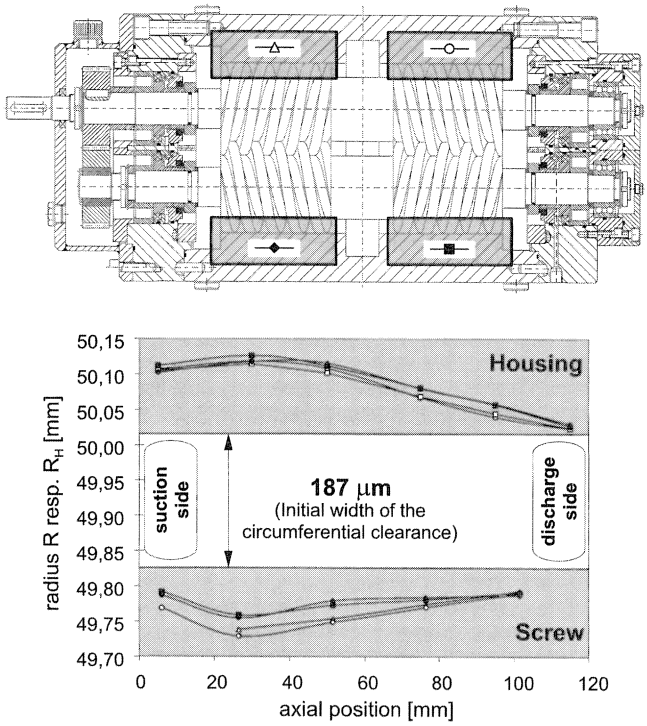

Figure 25. Local Wear of the Screw Package.

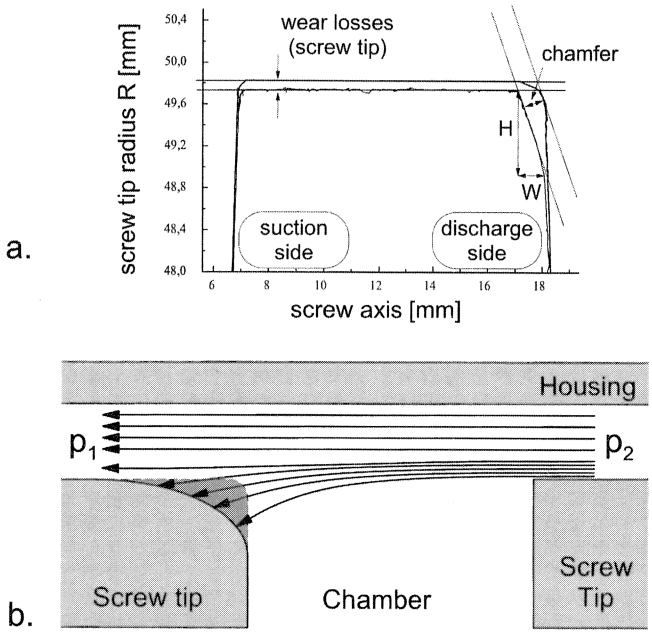

Figure 26. Local Wear at the Screw Tips.

Wear Hypothesis and Simulation

Based on the parameter study about the hydroabrasive wear in clearances (refer to Table 4), a correlation has been developed to compute and predict the pump's wear rates from RC tribometer tests (Schmidt, 1999).

$$W_l = W_{l,RCT} \cdot \frac{d_{Pm}}{d_{Pm,RCT}} \cdot \frac{c_p}{c_{P,RCT}} \cdot \frac{\dot{V}}{\dot{V}_{RCT}} \cdot 0.65 \cdot \left(\frac{s}{s_{RCT}}\right)^{(-1.1)} \cdot \left(\frac{\sqrt{\upsilon_{ax}^2 + \upsilon_{circ}^2}}{\upsilon_{RCT}}\right)^{2.93} \cdot M_R \quad (30)$$

This formula is based on the obvious expectation that a fluid's consistency remains constant everywhere in the pump and over all the time. The terms with the index RCT represent the RC tribometer data.

But as all attempts failed to properly predict the hydroabrasive pump wear with the correlation (Equation (30)), and due to the unexpected experience that the wear rate does not remain constant, the screw studies were performed to find a suitable hypothesis.

As deflection and eccentricity of the screw turned out to have no effect on wear, and other traces were ineffective at solving the problem (Schmidt, 1999), the assumption of a gradient of the particle concentration in the suspension as well as a nonuniform size distribution of the abrasive particles over the length of the screw package appeared a quite promising step.

From other observations (Idelchik, 1986), the formation of vortices in labyrinth seals is well known. As the geometry of the cross section of the spindles is quite similar to such geometric conditions, the presence of similar flow patterns in the conveying chambers is quite likely.

As a first approach, the development of simple vortices in the chambers is assumed (Figure 27). The separating effect makes the coarser particles move in a radial direction, joining the axial leak flow through the circumferential clearances.

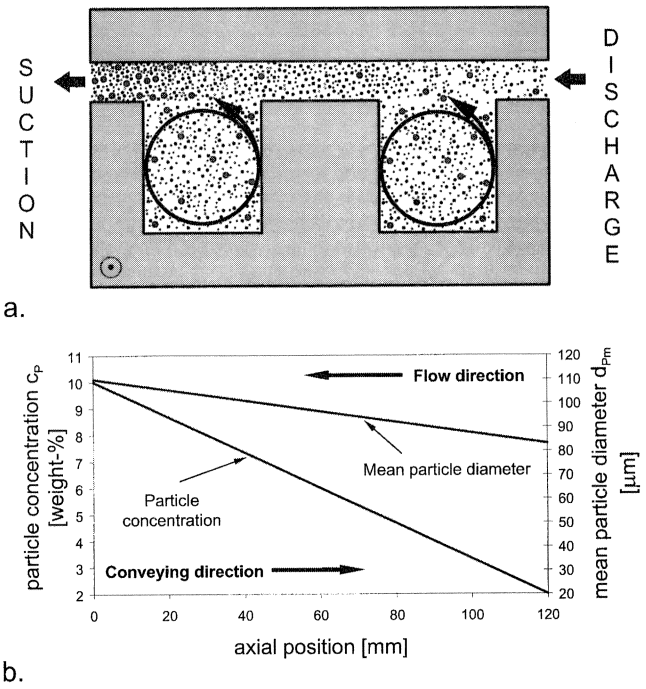

Figure 27. Principle of the Chamber Vortex Hypothesis (a) and Assumed Gradients of Particle Size and Concentration (b).

This implements a continuous increase of particle concentration and medium particle size toward the suction side of the pump. A comparable separation process is also triggered by the rotation of the screws and the involved centrifugal forces involved.

An iterative computation of the wear losses based on a combination of Equation (30) and the assumption of the Chamber Vortex Hypothesis is realized in the computer program SPALTCON (Schmidt, 1999).

The application of this program code is demonstrated at the wear patterns observed in the field test described above (screw: X35 CrMo 17, WNr. 1.4122, similar S 42080, plasma nitrided; bushing: X35 CrMo 17, WNr. 1.4122, similar S 42080). The assumptions were made that the slurry concentration in the clearances decreases from 10 weight percent (suction side) toward 2 weight percent (discharge side), and the medium particle size decreases from 110 µm (suction side) to 83 µm (discharge side).

Please note: The stated assumptions have been chosen quite arbitrarily because there is actually no proof on an experimental basis available.

Figure 28 shows the comparison of the measured wear losses after the wear tests and the calculated losses computed by means of the Chamber Vortex Hypothesis based on the hypothetical assumptions.

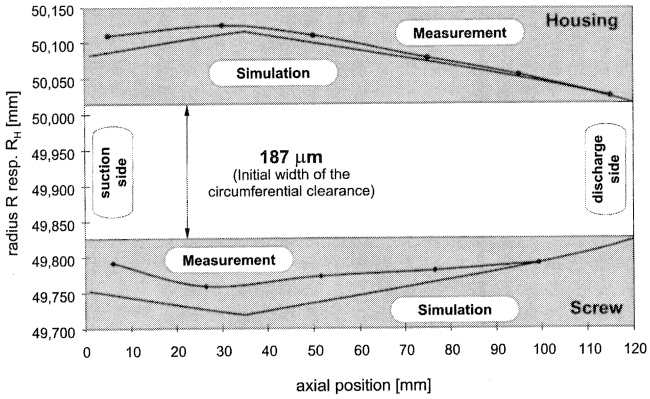

Figure 28. Comparison of Measured and Computed Wear Losses.

The simulated losses at the discharge side of the housing correspond well with the measured values. The region near the suction side shows some aberrations.

It should be noted clearly that the program code used is not practically capable to predict the pump's wear rates actually, because in reality most of the required data are not available and the assumptions on which the computer simulation is based represent only one of many scenarios imaginable.

The effective value of the computer program approach is that the computer simulation can basically be achieved and that, together with reasonable assumptions, the computational predictions seem to strengthen the Chamber Vortex Hypothesis and explain the unexpected wear rate distribution along the screws. This should encourage further research to continue on this trace.

CONCLUSION

Experimental and theoretical studies clearly demonstrate the twin screw pump's suitability for multiphase pumping services. The positive displacement pump type is capable of conveying oil/gas mixtures up to gas void fractions of 95 percent and more with good performance and efficiency.

The theoretical modeling of the twin screw pump's hydrodynamics has achieved impressive maturity, due to the various analytical steps with respect to the clearances' leak losses, the real clearance geometry during operations, and the thermodynamics close to isothermal change of state.

The new MEFAP computer code predicts the pump's reality satisfactorily well within the whole range of technical applications. The assumptions implemented into the pump modeling have been verified by extended experimental studies. The experimental evaluation of the pressure distributions along the screw package provides a proper understanding of the twin screw pump characteristics during multiphase service.

To the fact that the pump's capacity is starting to break down at gas void fractions above 96 percent should be responded to by liquid injection devices.

The studies of the hydroabrasive wear during the attack of hard particle contamination of the pumping fluid provide a close insight about the potential and kind of wear protective steps.

The tribometric simulation of the most important circumferential clearances in twin screw pumps yields a very effective tool to find positive steps for the extension of the pump's life-cycle. The important result is that the relative suitability of materials is indicated equally by the rotary clearance tribometer and the pump field test.

A number of hard wear resisting materials have been tested and experienced, including coatings or surface treatments on thermal and thermochemical bases.

The 3D determination of the local hydroabrasive wear rates in twin screw pumps has provided evidence about the real tribological situation and guided the first steps toward a computer aided wear or lifetime prediction.

NOMENCLATURE

Latin

A	(m^2)	Cross section
a	(m)	Distance between the axis
B	(m)	Width of the screw profile
c_P	(weight-%)	Particle concentration
D	(m)	External diameter of the screw
D_H	(m)	Internal diameter of the housing (bushing)
d	(m)	Internal diameter of the screw
d_P	(µm)	Particle size
d_{Pm}	(µm)	Mean particle size
F	(m^2)	Area flank clearance
f	(m^2)	Area to calculate F
G	(-)	Number of threads
g	(-)	Number of full stages
H	(m)	Chamber depth
H	(mm)	Height of screw tip chamfer
HV_M	(-)	Vickers hardness of the materials
HV_P	(-)	Vickers hardness of the particles
h	(m)	Pitch of the screw
K	(-)	Roughness factor
k	(-)	Number in general, number of stages
l_{CC}	(m)	Length of the circumferential clearance
l_{FC}	(m)	Active length of the flank clearance
l_f	(m)	Length of F
l_S	(m)	Length of the screw
M_R	(-)	Meshing ratio
N	(-)	Polytropic exponent
n	(min^{-1})	Pump speed
p	(bar)	Pressure
p_S	(bar)	Suction pressure
p_D	(bar)	Discharge pressure
Δp	(bar)	Pressure differential
R	(m)	External radius of the screw
R_H	(m)	Internal radius of the housing (bushing)
R_h	(-)	Hardness ratio
R_t	(µm)	Mean surface roughness
r	(m)	Internal radius of the screw
s_{CC}	(m)	Width of the circumferential clearance
s_{FC}	(m)	Width of the circumferential flank clearance
s_0	(m)	Clearance
s_{RC}	(m)	Width of the circumferential radius clearance
$s(x)$	(m)	Variable width
T	(Nm)	Torque
T_D	(°K)	Discharge temperature
T_S	(°K)	Suction temperature
u	(m)	Circumferential velocity
$\dot{V}$	(m^3/h)	Volume flow
$\dot{V}_c$	(m^3/h)	Total leak flow through a clearance
$\dot{V}_{cd}$	(m^3/h)	Component of $\dot{V}_c$ due to differential pressure
$\dot{V}_{cr}$	(m^3/h)	Component of $\dot{V}_c$ due to rotational meshing
$\dot{V}_g$	(m^3/h)	Gas volume flow
$\dot{V}_{geo}$	(m^3/h)	Volume flow (geometrical)
$\dot{V}_L$	(m^3/h)	Leak flow
$\dot{V}_{L,D}$	(m^3/h)	Differential pressure component of a leak flow
$\dot{V}_{L,R}$	(m^3/h)	Rational meshing component of a leak flow
$\dot{V}_{liq}$	(m^3/h)	Liquid volume flow
V_u	(m^3)	Displacement volume per revolution
v	(m/s)	Flow velocity (average)
v_{ax}	(m/s)	Axial flow velocity
v_{circ}	(m/s)	Circumferential flow velocity
v_r	(m/s)	Flow velocity (average) due to rotation
v_{res}	(m/s)	Resulting flow velocity
W	(mm)	Width of screw tip chamfer
W_l	(mm/a)	Linear wear rate
w	(m)	Flow velocity (average)
x	(-)	Coordinate axis
x_0	(m)	Half effective length of radial clearance
y	(-)	Coordinate axis
z	(-)	Coordinate axis

Greek

α	(-)	Gas void fraction (suction)
α_s	(-)	Pitch angle (screw)
β	(-)	Angle of the screw profile
β_E	(-)	Angle of obliquity of action
δ	(-)	Fraction of a stage
η	(-)	Coordinate axis
η_{vol}	(-)	Volumetric efficiency
η_{isoth}	(-)	Isothermal efficiency
φ	(-)	Angle of rotation
λ_l	(-)	Dimensionless length of the screw
μ	(Pas)	Dynamic viscosity
μ_c	(Pas)	Dynamic viscosity of the mixture (clearance)
μ_{ch}	(Pas)	Dynamic viscosity of the mixture (chamber)
μ_g	(Pas)	Dynamic viscosity (gas)
μ_{liq}	(Pas)	Dynamic viscosity (liquid)
ρ	(kg/m^3)	Density
ρ_c	(kg/m^3)	Density of the mixture (clearance)
ρ_{ch}	(kg/m^3)	Density of the mixture (chamber)
ρ_g	(kg/m^3)	Density (gas)
ρ_{liq}	(kg/m^3)	Density (liquid)
τ_K	(s)	Existence time of a chamber
υ	(m^2/s)	Kinematic viscosity
ω	(s^{-1})	Angular velocity
ξ	(-)	Coordinate axis

REFERENCES

Christiansen, B., 1986, "Preliminary Tests of a Two-Phase Flow Pumping Using the Bornemann 7.2z-28 Screw Pump," University of Trondheim.

Ciccetti, A. and Lombard, D., 1960, "Two-Phase Cooling Experiments Pressure Drop, Heat Transfer and Burnout Measurements," Energia Nucleare 1960, *7*, (6), p. 407 ff.

Cordner, M., July 1994, "Multiphase Pumps for Marginal Oil Field," *World Pumps*, p. 38 ff.

Dal Porto, D. F. and Larson, L. A., 1996, "Multiphase Pump Field Trials—Demonstrate Practical Applications for the Technology," SPE Annual Tech. Conf. and Exhib., Denver, Colorado, (Synopsis IPT, p. 927).

de Salis, J., April 1997, "Multiphasenpumpen Bekommen Keinen Schluckauf," *Sulzer Technical Review*, S. 10 ff.

Dosing Handbook, 1998, "Dosing of Liquids with Metering Pumps," Chapter 4, Vetter, G. (Ed.), Oxford, England: Elsevier Adv. Techn.

Granato, M., Colombi, P., and Ferrari Aggadi, G., September 1998, "Two Years of Testing the Two-Phase Pump," *Quadernipignone* 64, p. 16 ff.

Hamelberg, F. W., 1968, "Untersuchungen an Pumpen-Läuferprofilen, Läuferkräften und Leistungen von Schraubenpumpen," VDI-Forschungsheft 527.

Höppel, H. W., 1997, "Schädigungsmechanismen und Hydroabrasives Verschleißverhalten Unterschiedlicher Hartstoffsysteme," Dissertation, Universität Erlangen-Nürnberg.

Höppel, H. W., Mughrabi, H., Sockel, H. G., Schmidt, S., and Vetter, G., 1999, "Hydroabrasive Wear Behaviour and Damage Mechanisms of Different Hard Coatings," Wear 225-229, p. 1088 ff.

Idelchik, I. E., 1986, *Handbook of Hydraulic Resistance*, Berlin, Germany: Springer Verlag, pp. 92-96.

Kießling, R., 1994, "Zur Modelierung und Simulation des hydroabrasiven Verschleißes ringförmiger Strömungsspalte," Dissertation, Universität Erlangen-Nürnberg.

Körner, H., 1998, "Zum Förderverhalten von Schraubenspindelpumpen für Zweiphasen-Gemische hohen Gasgehalts," Dissertation, Universität Erlangen-Nürnberg.

Neumann, W., 1992, "Multiphasentransport mit Schraubenspindelpumpen," *Pumpen*, Vetter, G. (Ed.), Vulkan-Verlag Essen, S. 7 ff.

NN Westinghouse Electric Company, 1999, "WELLAMPS™ Subsea Multiphase Pumping System."

Prang, A., November 1981, "Rotary Screw Pumps for Multiphase Products," *World Pumps*, p. 19 ff.

Schmidt, S., 1999, "Verschleiß von Schraubenspindelpumpen beim Betrieb mit Abrasiven Fluiden," Dissertation, Universität Erlangen-Nürnberg.

Vetter, G. and Kießling, R., 1996, "Zur Auslegung von Spaltdichtungen in Pumpen gegen hydroabrasiven Verschleiß," Konstruktion 48, p. 167 ff.

Vetter, G. and Körner, H., 1998, "Computer Program MEFAP," Universität Erlangen-Nürnberg, Department of Apparatus and Chemical Machinery.

Vetter, G. and Wincek, M., 1993a, "Performance Prediction of Twin-Screw Pumps for Two-Phase Gas/Liquid Flow," Pumping Machinery ASME, *154*, p. 331 ff.

Vetter, G. and Wincek, M., 1993b, "Zum Förderverhalten von Schraubenspindelpumpen bei der Förderung von Flüssigkeits/Gas-Gemischen," Konstruktion 45, p. 203 ff.

Vetter, G., Kießling, R., and Wirth, W., 1996, "Abrasive Wear in Pumps—A Tribometric Approach to Improve Pump Life," *Proceedings of the Thirteenth International Pump Users Symposium*, Turbomachinery Laboratory, Texas A&M University, College Station, Texas, pp. 143-158.

Wincek, M., 1992, "Zur Berechnung des Förderverhaltens von Schraubenspindelpumpen bei der Förderung von Flüssigkeits/Gas-Gemischen," Dissertation, Universität Erlangen-Nürnberg.

Wincek, M. and Moser, W., 1999, "Subsea—Ein neues Anwendungsgebiet für die Mehrphasenschraubenpumpe," Industriepumpen + Kompressoren, Heft 2, S. 93 ff.

Zum Gahr, K. H., 1990, "Modeling of Microstructural Effects on Abrasive Wear," *Microstructure and Mechanical Properties*, Tenkhoff, E. and Vöhringer, O. (Ed.), DGM Informationsgesellschaft, Oberursel, p. 171 ff.